Stanford Exploration Project, Report 115, May 22, 2004, pages 249–264

First-order lateral interval velocity estimates without picking

Antoine Guitton, Jon Claerbout, and Jesse Lomask[1]

ABSTRACT

A new method for estimating interval velocities without picking is proposed. The first step applies a normal move-out correction with a $v(z)$ stacking velocity to common mid-point gathers. The second step estimates local stepouts at every offset and time for each gather. Local stepouts across offset are then integrated to obtain local time shifts. The integration is done in the Fourier domain for increased speed. Finally the interval velocity is estimated in the τ space by fitting the time shifts with a tomographic inversion procedure based on a straight rays geometry. This approach is tested on a Gulf of Mexico dataset with flat geology where recovery of lateral velocity variations across faults is demonstrated.

INTRODUCTION

Interval velocity estimation requires picking in many circumstances. For example, one might pick parameters indicating the flatness of a common depth point (CDP) gather for an initial velocity model (Al-Yahya, 1989; Etgen, 1990) or how well an image focuses after residual migration (Biondi and Sava, 1999). Stereotomography (Billette et al., 2003) requires picking slopes and traveltimes for the velocity estimation process. Other imaging techniques such as common-focus-point migration involve semblance analysis for updating focusing operators (Berkhout and Verschuur, 2001). Moreover, for most of these methods, specifically those based on tomography, several reflectors need to be selected (picked) for the velocity inversion (Clapp, 2001).

Very few velocity estimation techniques do not require any picking. For instance, Toldi (1989) derives a relationship between interval and stacking slowness perturbations that is valid for flat geology with constant velocity background. Closest to our approach, Symes and Carazzone (1991) directly invert time shifts between adjacent traces to estimate interval velocities.

It is our belief that picking is inherently flawed and should be replaced by more robust techniques requiring as little human interpretation as possible. The major shortcomings of human intervention are unrepeatability and subjectivity. Results of velocity analysis invariably differ from one person to another based on the tools used to perform the picking or on the experience of the interpretor. Our conjecture is as follows:

[1]**email:** antoine@sep.stanford.edu, jon@sep.stanford.edu, lomask@sep.stanford.edu

It is difficult to pick arrivals or events at different spatial locations reliably. However, it is easy to estimate local stepouts between adjacent traces. Event picking should always be replaced by dip estimation.

Therefore, we propose a fully automated interval velocity estimation technique based on (1) dip estimation, (2) dip integration and (3), tomographic inversion. The ultimate goal of this work is to be able to provide a robust technique that affords a first order estimate of interval velocities.

The initial velocity, or starting guess, is a $v(z)$ model. From this simple model we apply a NMO correction to the CMP gathers. In general, NMO is unable to completely flatten CMP gathers because of laterally varying velocity. Flat gathers are then obtained by estimating a trace-by-trace local stepout from the NMO corrected gathers. Local stepouts are then integrated to form absolute time shifts at every time, offset, and midpoint location. If data are noise-free (bad traces, random noise), estimated time shifts flatten gathers regardless of the subsurface complexity.

Time shifts are then used to perform a tomographic inversion in (x, τ) space (Clapp and Biondi, 2000), where x is the mid-point position and τ the zero-offset travel time. Straight rays are assumed between the subsurface location and the source/receiver positions; however, this assumption is evidently violated for any realistic geological setting. We none-the-less show that this simplistic model leads to a reasonable velocity update.

Once the interval velocity is updated, more iterations of tomography are usually required. Because of the assumptions made in the tomographic inversion, we stop at the first velocity update. One way to check whether the estimated velocity perturbations flatten the gathers or not is by applying the forward modeling operator to the estimated velocity perturbations; the modeled time shifts can then be applied to the NMO corrected gathers. From this approach we are able to obtain updated interval velocities and flat CMP gathers. In the next two sections, the time-shifts estimation step and the tomographic inversion are described.

ESTIMATION OF TIME SHIFTS

Estimating time shifts is a two step procedure where local stepouts are first estimated and then integrated. The goal of dip estimation is to find a local stepout, p_h, that destroys the local plane wave such that,

$$0 \approx \frac{\partial u}{\partial h} + p_h \frac{\partial u}{\partial \tau}, \tag{1}$$

where u is the wavefield at time τ, midpoint x and offset h. For all gathers, we evaluate the slope p_h with a method based on high-order plane-wave destructor filters (Fomel, 2002). This technique has the advantage of being accurate for steep dips. The estimation of p_h is based on a non-linear algorithm (Gauss-Newton method) that includes a regularization term. This regularization smooths dips across offset and CMP location. One problem with the current technique is that the dip estimation algorithm cannot properly handle conflicting dips. This

can be troublesome when, for instance, multiples are present in the data. To solve this problem, Fomel (2002) and Brown (2002) show how two dips can be estimated. Then if multiple reflections are present, the stepouts corresponding to the primaries are kept and those of the multiples are rejected.

Dips estimates lead to a vector of local stepouts $\mathbf{p}_h$ that are integrated one CMP at a time to obtain time shifts. Dips are smoothed along both spatial directions but not in time τ. To enforce smoothness in the τ direction Lomask and Guitton (2004) introduce a time component $\mathbf{p}_\tau$ to $\mathbf{p}$. The relationship between the local time shift vector, $\mathbf{t_s} = \mathbf{t_s}(\tau, x, h)$ and the local dip vector $\mathbf{p} = (\mathbf{p}_h, \mathbf{p}_\tau)^T$ $((.)^T$ being the transpose) at a constant x is:

$$\mathbf{p} = \begin{pmatrix} \mathbf{p}_h \\ \mathbf{p}_\tau \end{pmatrix} = \begin{pmatrix} \partial_h \mathbf{t_s} \\ \partial_\tau \mathbf{t_s} \end{pmatrix}, \tag{2}$$

where ∂_τ and ∂_h are the partial derivative in τ, h respectively. In practice, we choose $\mathbf{p}_\tau = \mathbf{1}$ and control the amount of smoothness by introducing a trade-off parameter ϵ as follows (Lomask and Guitton, 2004):

$$\begin{pmatrix} \partial_h \mathbf{t_s} \\ \epsilon \partial_\tau \mathbf{t_s} \end{pmatrix} = \begin{pmatrix} \mathbf{p}_h \\ \epsilon \mathbf{p}_\tau \end{pmatrix}. \tag{3}$$

Using equation (3) we wish to minimize the length of a vector $\mathbf{r_{t_s}}$ that measures the difference between $\mathbf{p}_\epsilon$ and $\nabla_\epsilon \mathbf{t_s}$ as follows:

$$\mathbf{0} \approx \mathbf{r_{t_s}} = \nabla_\epsilon \mathbf{t_s} - \mathbf{p}_\epsilon, \tag{4}$$

where $\nabla_\epsilon = (\partial_h, \epsilon \partial_\tau)^T$, and $\mathbf{p}_\epsilon = (\mathbf{p}_h, \epsilon \mathbf{p}_\tau)^T$. We then minimize the following objective function:

$$f(\mathbf{t_s}) = \|\mathbf{r_{t_s}}\|^2, \tag{5}$$

where $\|.\|$ is the L_2 norm. By increasing ϵ, the estimated time shifts $\hat{\mathbf{t}}_\mathbf{s}$ become smoother in time. We solve equation (5) analytically in the Fourier domain (Lomask, 2003), which speeds up the estimation of $\mathbf{t_s}$:

$$\hat{\mathbf{t}}_\mathbf{s} \quad = \quad \mathrm{FFT_{2D}}^{-1} \left[\frac{\mathrm{FFT_{2D}} \left[\nabla'_\epsilon \mathbf{p}_\epsilon \right]}{-Z_h^{-1} - \epsilon Z_\tau^{-1} + 2 + 2\epsilon - Z_h - \epsilon Z_\tau} \right] \tag{6}$$

where $Z_h = e^{iw\Delta h}$ and $Z_\tau = e^{iw\Delta\tau}$. The dip integration yields the desired time shifts plus a constant, i.e., a DC frequency component. The zero frequency component is removed by subtracting the near offset panel from the other offsets. Therefore, the time shifts are a measure of the moveout errors relative to the near-offset panel. At the end of the dip integration process, we end up with a map of time shifts, $t_s(\tau, x, h)$. These time shifts can be used to flatten the CMP gathers without any velocity analysis. Our goal, however, is to find an interval velocity function consistent with the estimated time shifts using a tomographic inversion procedure.

TOMOGRAPHY

From the time shifts, we estimate interval velocities in the τ domain. As pointed out by Alkhalifah (2003) and Clapp (2001), τ tomography is more robust than depth tomography to reflector position and velocity errors. However, going from depth to vertical travel time introduces new variables. As described by Biondi et al. (1997) and Alkhalifah (2003), the transformation from depth coordinates (x,z) into vertical-traveltime coordinates $(\tilde{x},\tau)$ is governed by the relationships:

$$\begin{aligned} \tau(x,z) &= \int_0^z \frac{2}{v(x,z')} dz', \\ \tilde{x}(x,z) &= x. \end{aligned} \tag{7}$$

Therefore, we have the following relationships between the differential quantities (dx,dz) and $(d\tilde{x},d\tau)$:

$$\begin{aligned} dz &= \frac{v(x,z)}{2} d\tau - \frac{v(x,z)\sigma}{2} d\tilde{x}, \\ dx &= d\tilde{x}, \end{aligned} \tag{8}$$

where $v(x,z)$ is the focusing velocity proportional to the mapping velocity (Clapp, 2001) and

$$\sigma = \int_0^z \frac{\partial}{\partial x}\left(\frac{2}{v(x,z')}\right) dz'. \tag{9}$$

In this paper, it is assumed that $x = \tilde{x}$ and $\sigma = 0$ because the initial slowness field is horizontally invariant.

The data space for this inverse problem is a cube of time-shifts at every time, offset and midpoint location. This differs from most tomographic techniques where a few reflectors are usually selected and picked for the inversion. The number of the model space unknowns (the velocity update) is the product of the number of gathers and the number of time samples. A velocity perturbation is computed for each pixel in the model space. For a CMP location x at time τ and offset h, a total time shift t_s is estimated. The forward problem relating velocity perturbation and time shift is derived from Fermat's principle:

$$t_s(\tau,x,h) = \int_0^\tau (\Delta s^-(r) + \Delta s^+(r)) dr, \tag{10}$$

with

$$dr = \frac{d(dt)}{dS}, \tag{11}$$

where $\Delta s^-(r)$ and $\Delta s^+(r)$ are the slowness perturbations along the down- and up-going rays respectively (from $x - h/2$ to x and $x + h/2$ to x), S is the focusing slowness, and dt the time increment along the ray (Clapp and Biondi, 2000). Note that slownesses are actually estimated and not velocities, as it is usually done in tomography. To simplify the problem, we assume that the up- and down-going rays are straight lines in the (τ,x) space.

Equation (10) is a linear relationship between the time shifts and the slowness perturbations allowing us to write,

$$\mathbf{d} = \mathbf{L}\mathbf{m}, \tag{12}$$

where $\mathbf{d}$ are the estimated time shifts, $\mathbf{L}$ is the tomographic operator in equation (10) and $\mathbf{m}$ is a field of slowness perturbations. Our goal is to find $\mathbf{m}$ such that,

$$\mathbf{0} \approx \mathbf{r_d} = \mathbf{L}\mathbf{m} - \mathbf{d}. \tag{13}$$

The addition of a regularization operator to enforce smoothness in the horizontal direction gives:

$$\begin{array}{rcrcl} \mathbf{0} & \approx & \mathbf{r_d} & = & \mathbf{L}\mathbf{m} - \mathbf{d}, \\ \mathbf{0} & \approx & \epsilon \mathbf{r_m} & = & \epsilon \nabla_x \mathbf{m}, \end{array} \tag{14}$$

where ∇_x is the horizontal gradient. Next, $\mathbf{m}$ is estimated in a least-squares sense by minimizing objective function,

$$f(\mathbf{m}) = \|\mathbf{r_d}\|^2 + \epsilon^2 \|\mathbf{r_m}\|^2. \tag{15}$$

In practice, $\mathbf{m}$ is estimated with a conjugate-gradient method and ϵ is estimated by trial and error. Because tomography is inherently non-linear, more iterations are needed to converge toward a satisfying velocity model. However, the assumptions made in this paper do not allow us to iterate without using more sophisticated imaging operators or ray tracing tools. We now test our method on a 2D Gulf of Mexico dataset.

A GULF OF MEXICO 2D FIELD DATA EXAMPLE

Figure 1 displays a near-offset section of a 2D dataset. The geology is relatively simple with mostly flat layers and few normal faults. A first 1D interval slowness model is estimated by assuming a $v(z) = v_0 + \alpha z$ function that leads to $v(\tau) = v_0 e^{\alpha \tau/2}$ in (x, τ) space. With this dataset $v_0 = 1.6 km/s$ and $\alpha = 0.5 s^{-1}$. We then transform the velocity into an interval slowness function shown Figure 2.

Figure 3 shows every twenty-fifth CMP gathers after NMO correction. Note that these gathers are not perfectly flat and that the noise level is quite high, especially in the deepest part of the section. In addition, there are both missing and bad traces at different offsets. We expect that the estimation of stepouts is robust enough to the noise level present in the gathers to give reasonable dips.

Local stepouts and time shifts are estimated from the CMP gathers. Figure 4 displays the estimated time shifts for the five selected CMP gathers. It is interesting to notice that the time shifts increase with offset. The time shifts are also relatively smooth in the τ direction thanks to the dip regularization in equation (3). The smoothing in both offset and midpoint directions during the stepouts estimation allows us to have time shifts where traces were originally

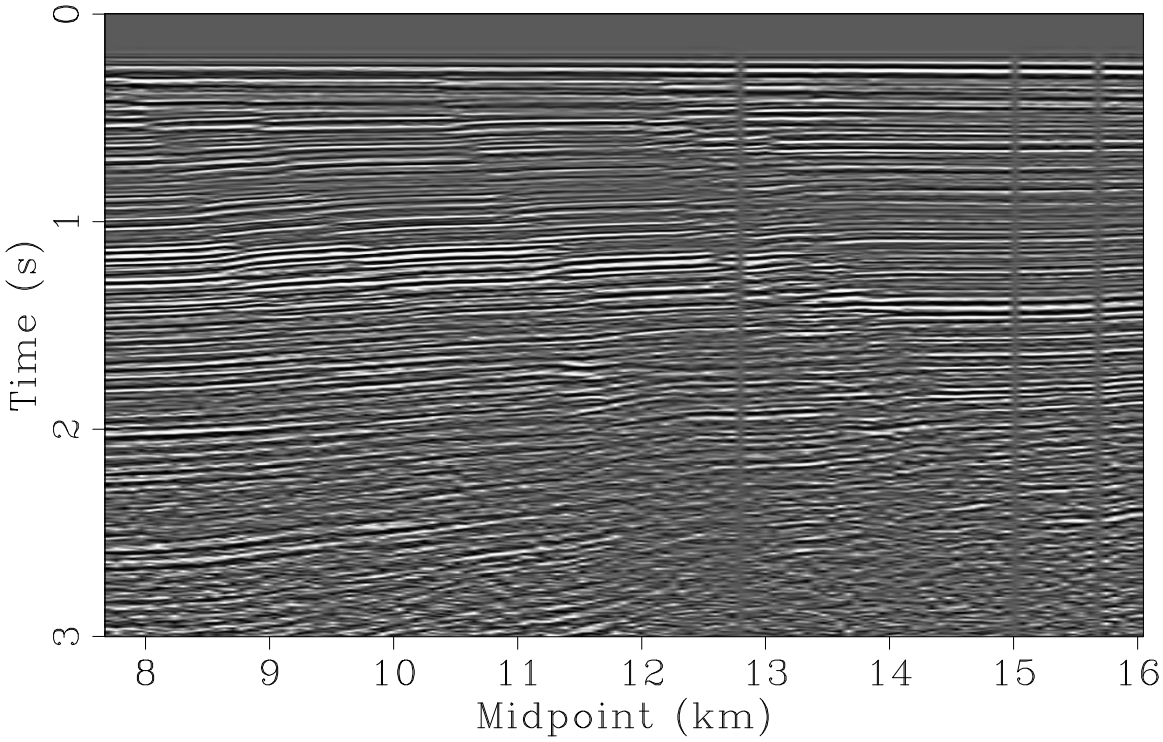

Figure 1: Near-offset section of the 2D field dataset from the Gulf of Mexico. Some normal faults are visible. antoine3-near-offset [ER]

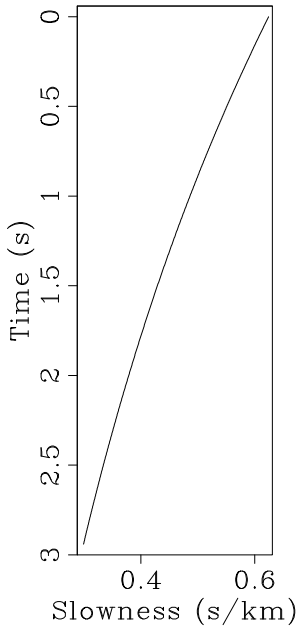

Figure 2: Initial slowness function. antoine3-s0 [ER]

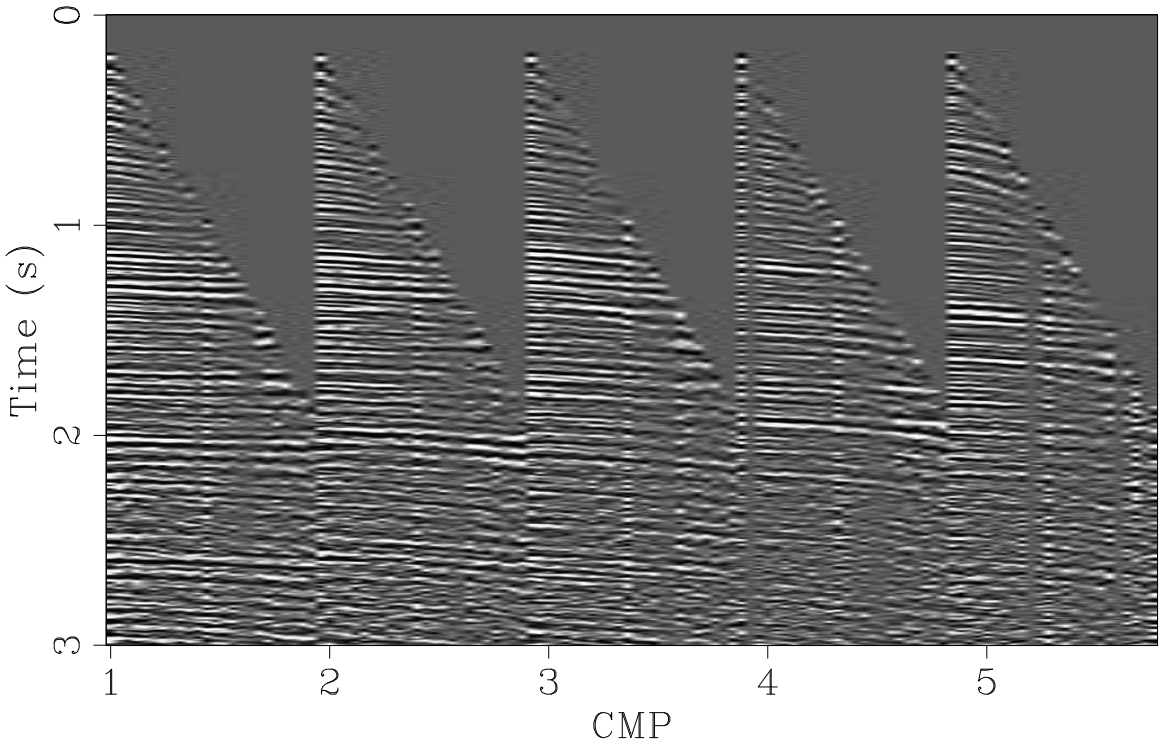

Figure 3: Five CMP gathers every 1.6 km after NMO correction with the RMS velocity derived from the interval slowness in Figure 2. Some residual curvature is apparent throughout the section. antoine3-pano.nmo [ER]

missing (e.g., gathers four and five in Figure 3). The fact that the estimated time shifts change with midpoint for a fixed time and offset prove that lateral velocity variations exist. These time shifts can be checked by applying a moveout correction to the input gathers in Figure 3 according to the shift values in Figure 4. Figure 5 shows the same gathers after moveout correction. These gathers are now flat and demonstrate that the estimated time shifts after integration of the local stepouts are correct.

The velocity perturbations are then estimated from the time shifts with the τ tomography. Figure 6 shows estimated slowness perturbations and Figure 7 displays the updated slowness field. We used 40 iterations and set $\epsilon = 1$ in equation (15) to obtain this result. Lateral velocity variations are visible throughout. In Figure 8, four fault locations interpreted from the seismic are superimposed (Figure 15). These faults locations seem to be aligned with velocity variations in Figure 7. In particular, it is pleasing to see the change of velocities across the different faults.

To check whether the method converged, modeled time shifts are estimated from the slowness perturbations in Figure 6 by applying the forward operator in equation (10). The re-modeled time shifts are shown in Figure 9. Comparing Figures 4 and 9, it appears that the re-modeled time shifts are smoother. Yet, applying these time shifts to the NMO corrected data in Figure 3 yield flat gathers (Figure 10). The difference between Figures 4 and 9 is

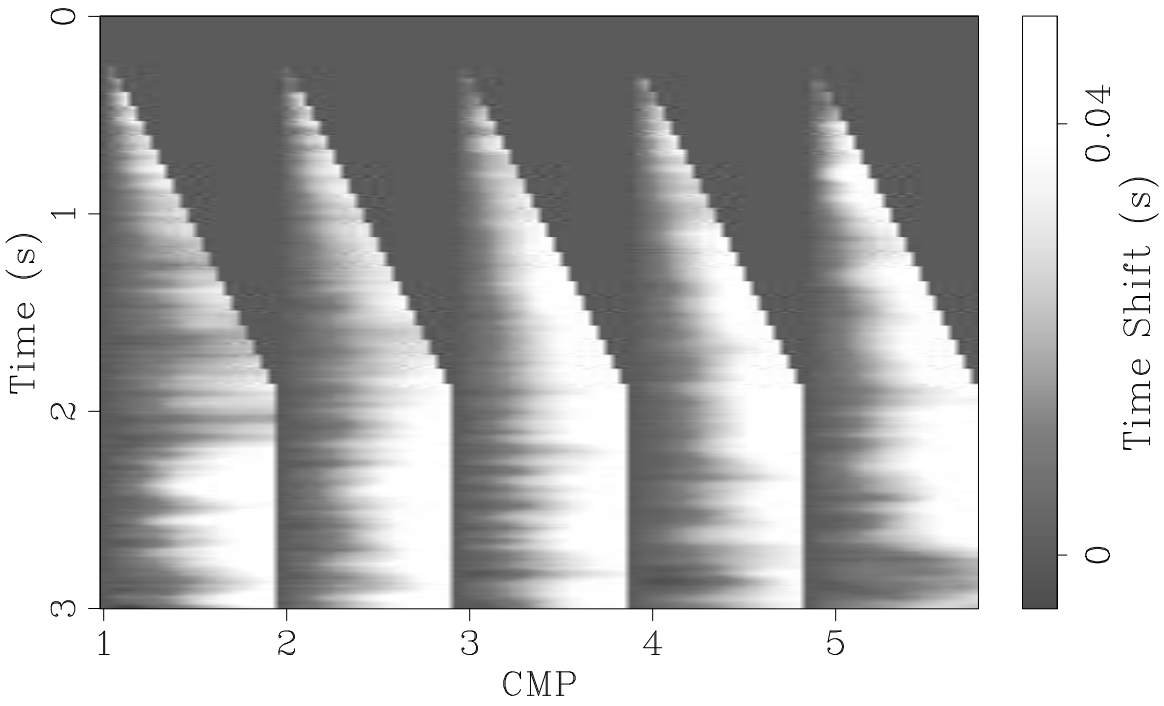

Figure 4: Estimated time shifts for five CMP gathers. The maximum time shift is around 0.05 s. Note that the first trace is set to zero. antoine3-time.pano.realshift [ER]

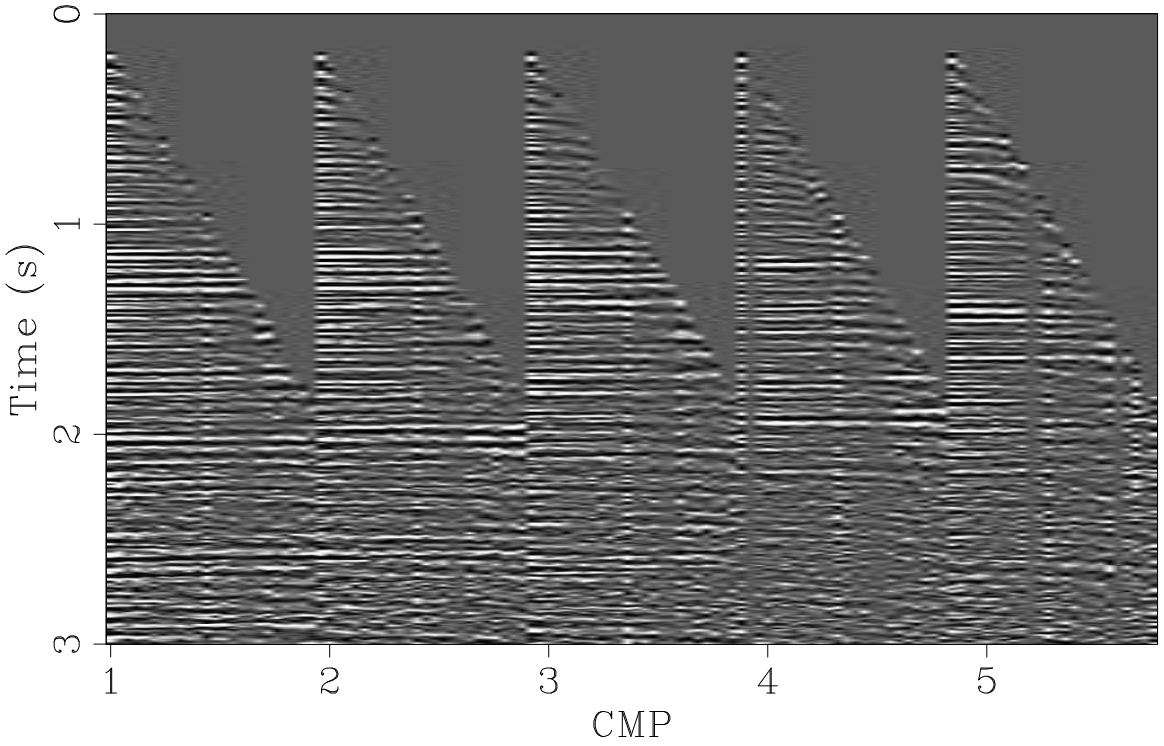

Figure 5: Flattened CMP gathers after applying the time shifts in Figure 4. Comparing with Figure 3, most of the events are now flat. antoine3-pano.data.flat [ER]

that the re-modeled time shifts are constrained by the physics of the tomographic inversion, thus giving well-behaved amplitude variations. In Figure 4, however, the time shifts take any value according to estimated dips. The forward operator of the tomographic inversion can be interpreted as a velocity-consistent, time shifts estimator.

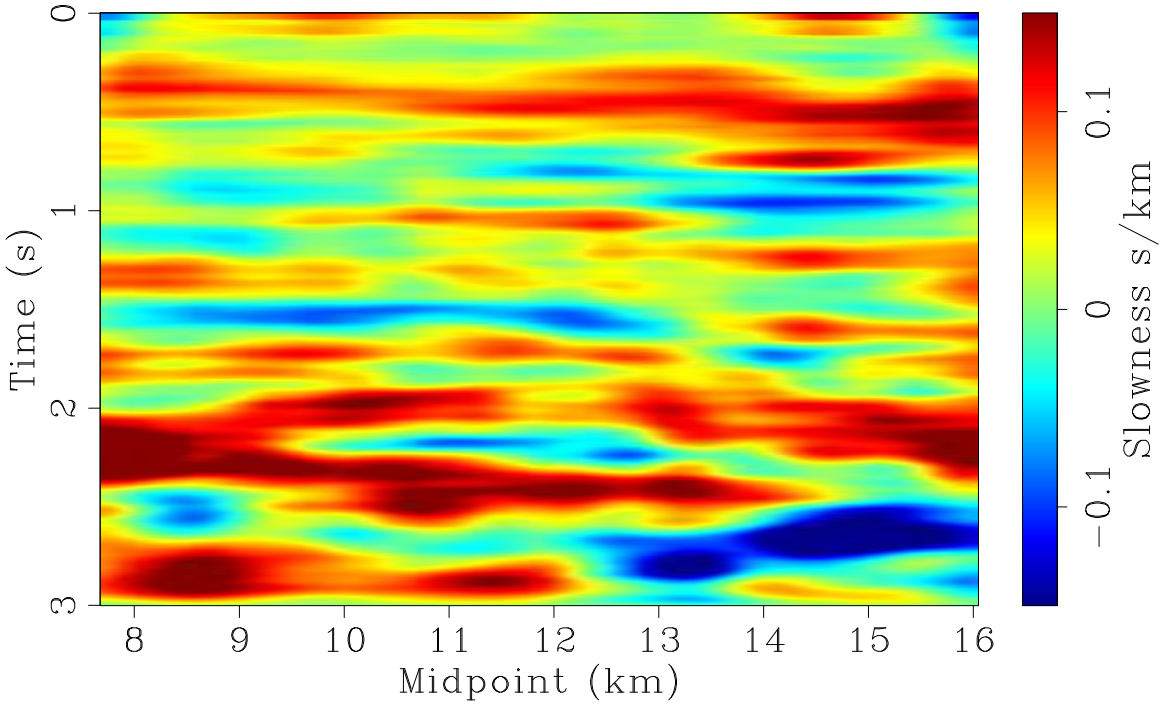

Figure 6: Slowness perturbations estimated from the tomography in the τ space. antoine3-delta.dslow [CR]

Finally, the flattened gathers in Figure 10 are stacked (Figure 14). We compare this result with the stacked section of the data with a 1D slowness model shown in Figure 11. This slowness function flattens the CMP gathers well for every midpoint position (Figure 12). We show the stacked section of the input data with this 1D slowness function in Figure 13. The reflectors are stronger and better defined in Figure 14 wherever the signal level is strong. In the lower part of the section, however, some continuous events in Figure 13 are attenuated in Figure 14. This effect is due to the difficulty to estimate meaningful stepouts when the noise level is too high. Again, four interpreted faults are shown on the stacked section in Figure 15.

DISCUSSION-CONCLUSION

We present a method for estimating interval velocities without picking. In this approach, we estimate time shifts from NMO corrected gathers by first computing local stepouts and then integrating them across offset. These time shifts are then fitted with a tomographic inversion in (x, τ) space. This approach seems to be robust to a reasonable noise level in the data. In addition, only a few parameters need to be chosen.

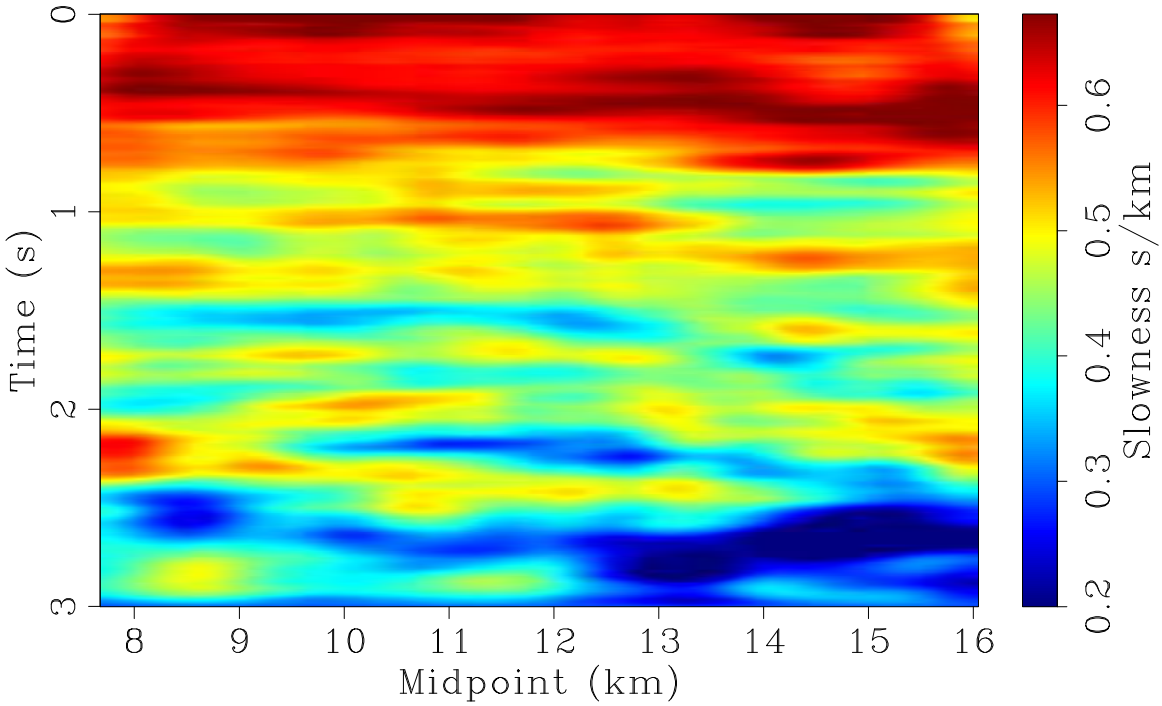

Figure 7: Updated slowness field by adding Figures 2 and 6. antoine3-vel.slowupdate [CR]

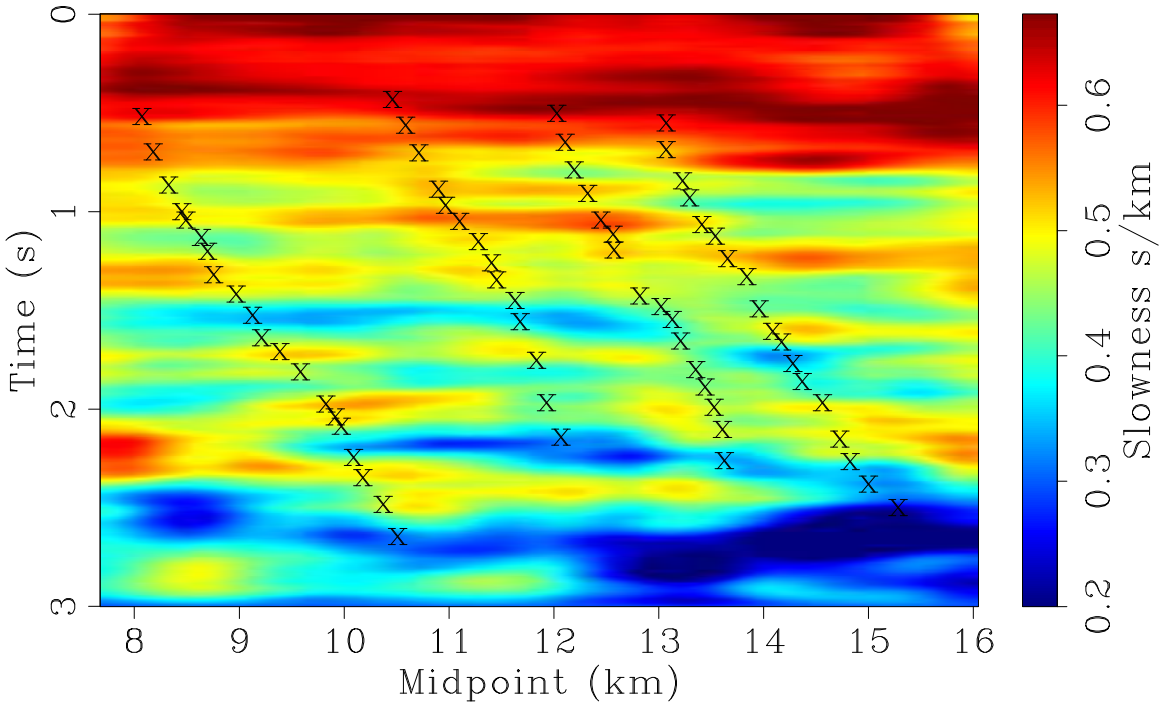

Figure 8: Same as Figure 7 with four interpreted faults from the seismic. Note the changes of velocity across the faults. antoine3-velinter.slowupdate [CR]

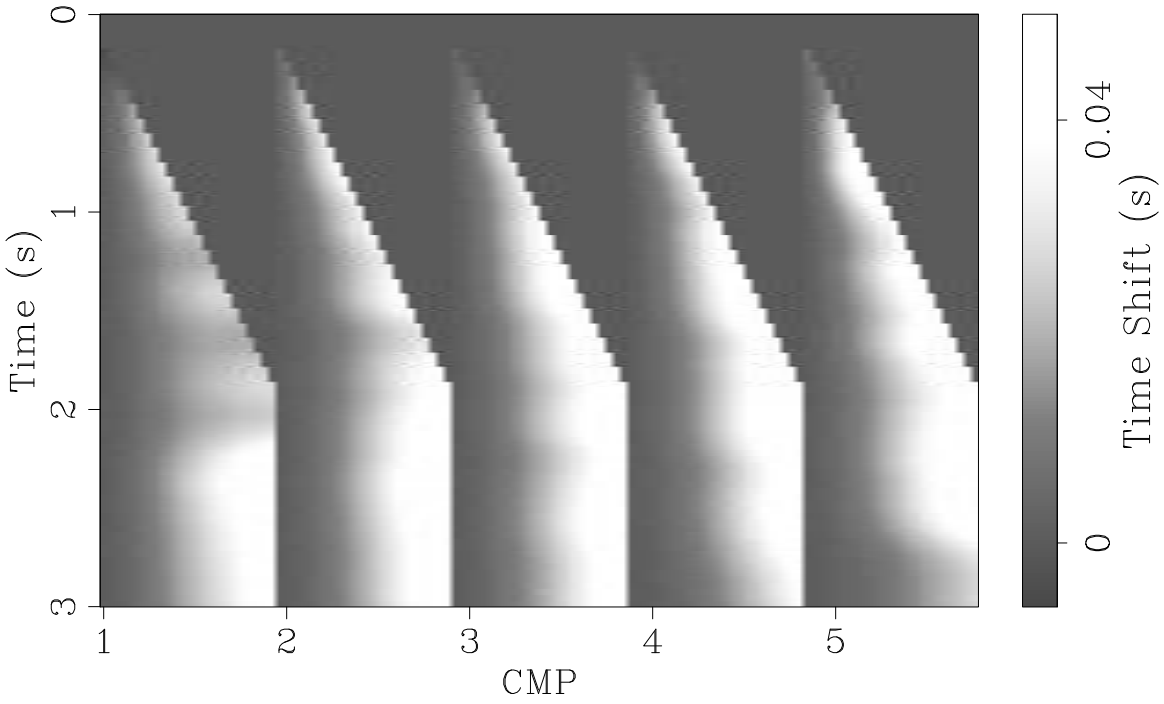

Figure 9: Modeled time shifts from slowness perturbations in Figure 6. Note that the remodeled time shifts are smoother than the original ones in Figure 4. antoine3-time.pano.newshift [CR]

This technique presents some limitations that require improvements. For instance the local stepouts need to be single valued with no conflicting dips in the data. This limitation can be overcome by estimating a few dips and retaining the ones of interest only. Second, an initial 1D velocity model is needed as a starting guess. This approximation, along with the simplified geometry of the rays, prevent us from recovering lateral velocity variations for complex geology, e.g., salt environment. This limitation can be overcome by incorporating the work of Clapp and Biondi (2000).

In spite of these approximations, this new velocity estimation technique is able to recover lateral velocity variations without picking for a 2D Gulf of Mexico dataset. In addition, the updated velocity field seems to match the geological environment: we can see velocity changes across faults at various locations. We finally show that the estimated velocity perturbations yield a map of time shifts that can be used to flatten CMP gathers.

In theory, more iterations of velocity updating should be performed. One problem with more updates is the need for more sophisticated time or depth imaging algorithms. In addition, more updates would mean improving on the tomographic inversion by allowing any type of ray geometry and background slowness field. These changes go beyond the scope of this paper. We believe, however, that all these sources of improvements should be investigated further to provide a robust and picking-free interval velocity estimation tool.

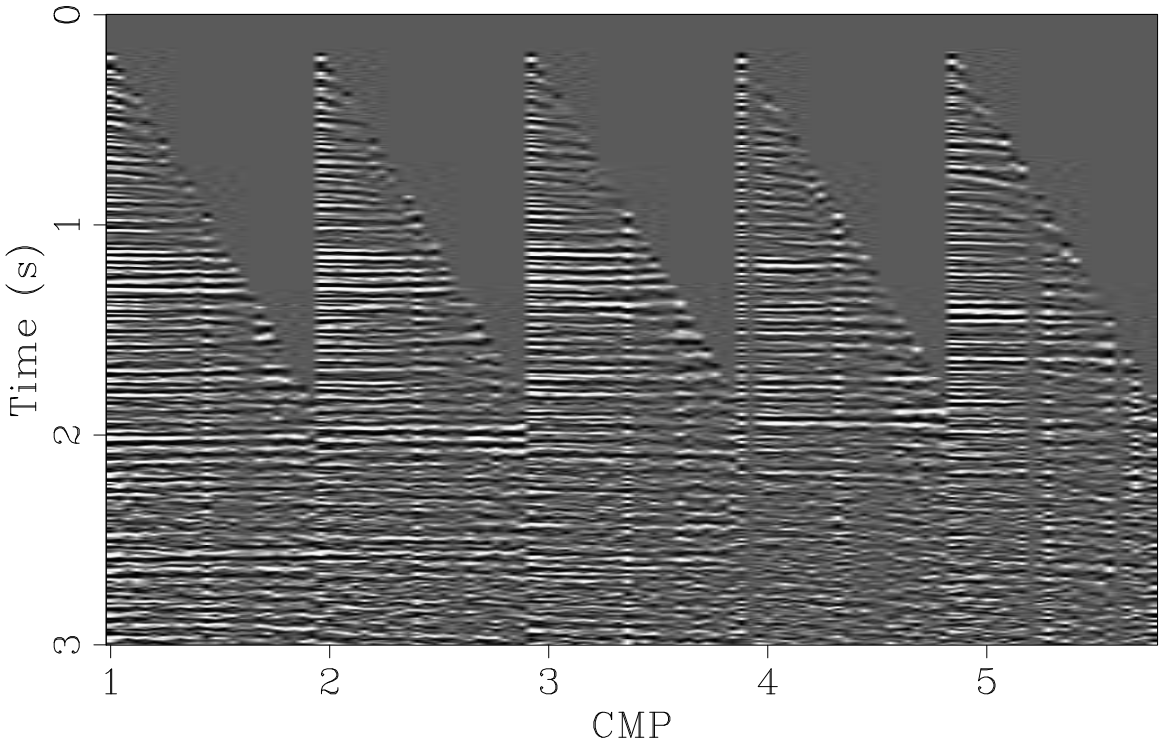

Figure 10: Flattened data with the remodeled time shifts in Figure 9. The gathers are flat showing that the slowness perturbations in Figure 6 fit the estimated time shifts in Figure 4 very well. antoine3-pano.new.data.flat [CR]

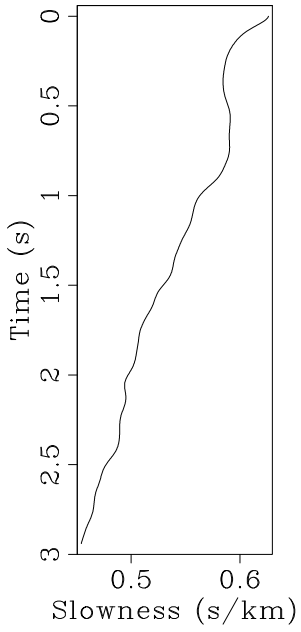

Figure 11: A 1D stacking slowness function. antoine3-s1 [ER]

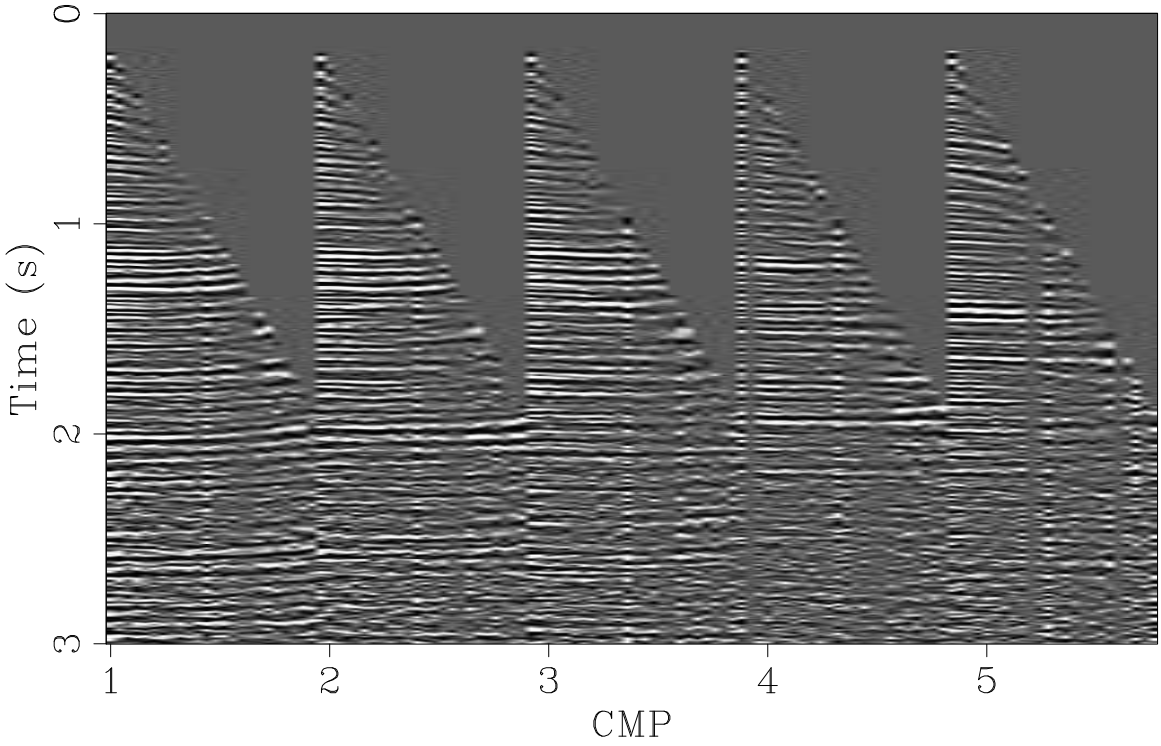

Figure 12: CMP gathers after NMO with the slowness function in Figure 11. The gathers are almost flat. antoine3-panos1 [ER]

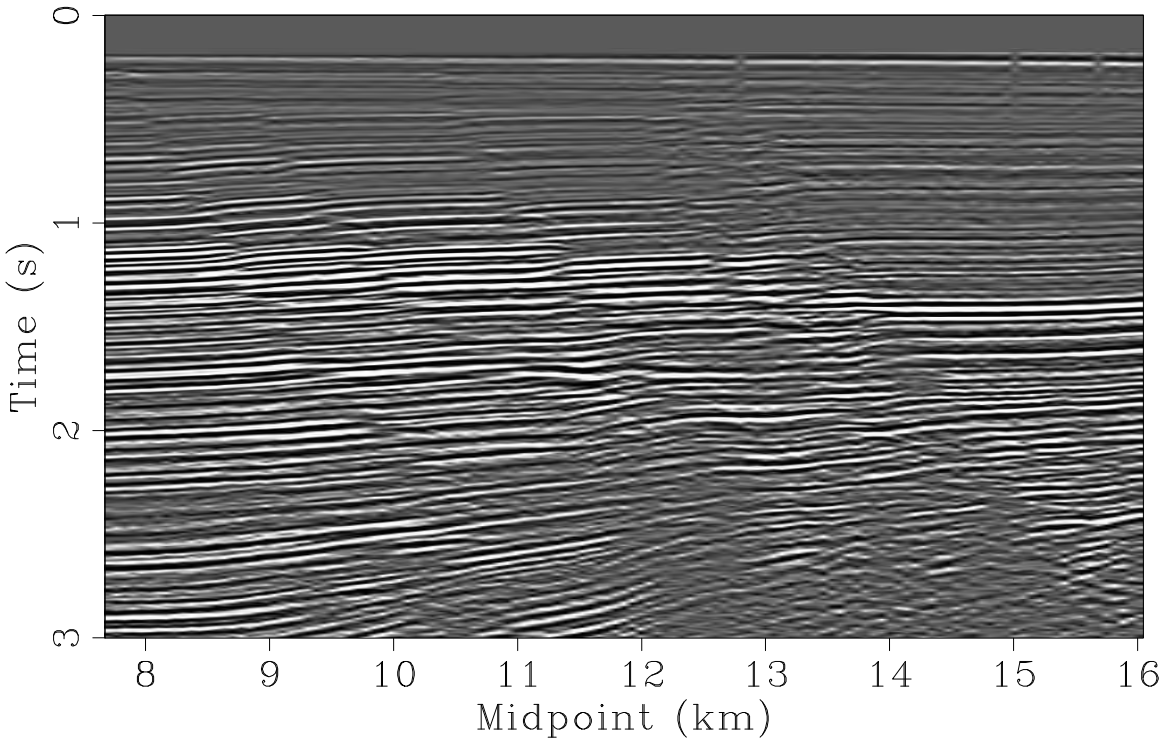

Figure 13: Stacked section of the data with the our best picked 1D slowness function in Figure 11. antoine3-stack-bestslow [ER]

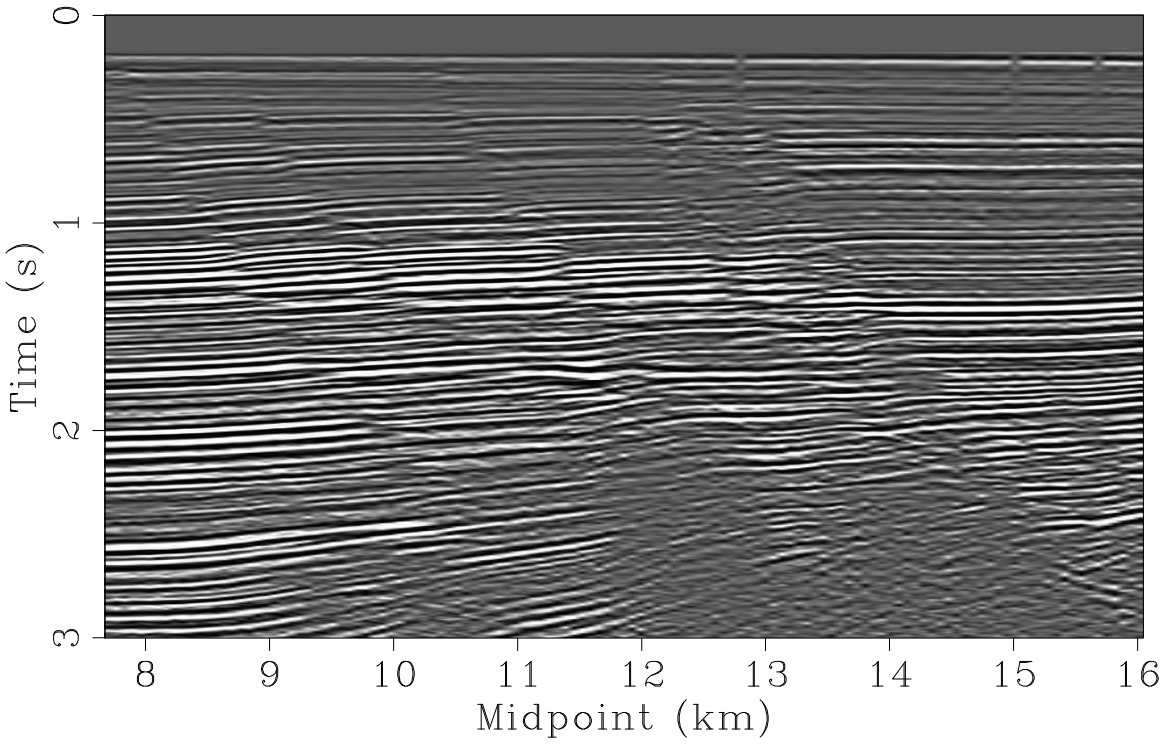

Figure 14: Stacked section of the moveout corrected data from the remodeled time shifts in Figure 9. antoine3-stack.new.data.flat [CR]

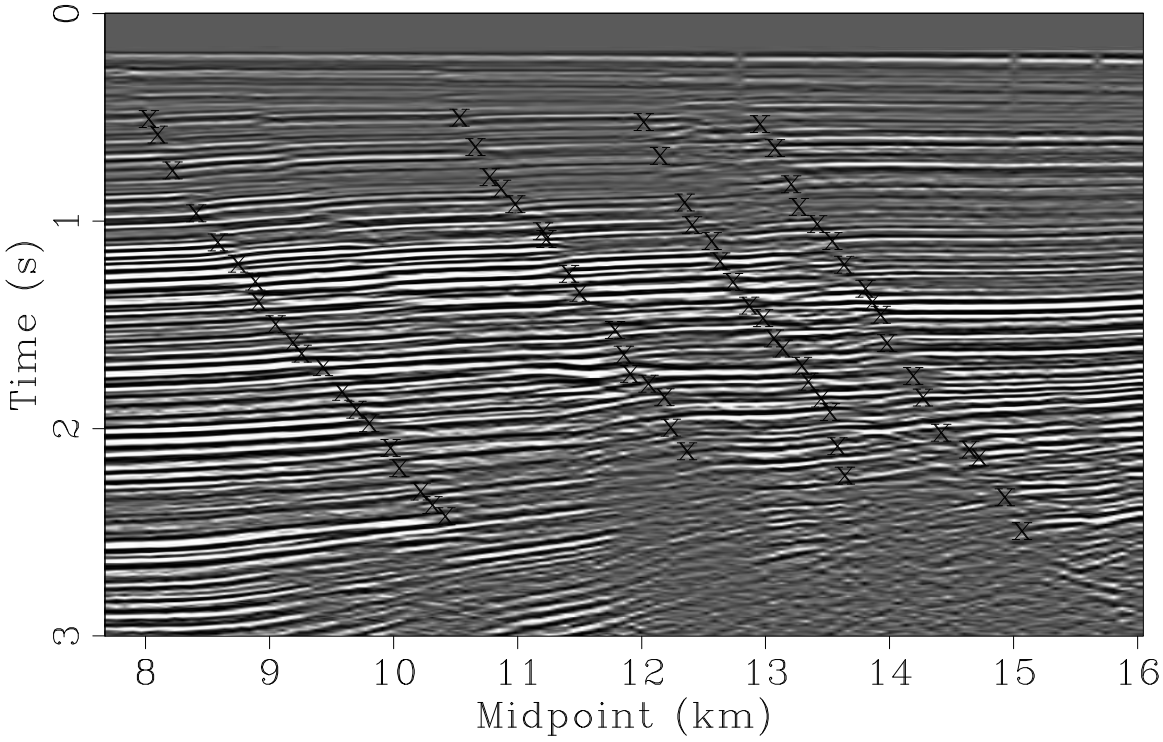

Figure 15: Stacked section of the moveout corrected data from the remodeled time shifts in Figure 9 with four picked faults. antoine3-stackinter.new.data.flat [CR]

REFERENCES

Al-Yahya, K. M., 1989, Velocity analysis by iterative profile migration: Geophysics, **54**, no. 06, 718–729.

Alkhalifah, T., 2003, Tau migration and velocity analysis: Theory and synthetic examples: Geophysics, **68**, no. 4, 1331–1339.

Berkhout, A. J., and Verschuur, D., 2001, Seismic imaging beyond depth migration: Geophysics, **66**, no. 6, 1895–1912.

Billette, F., Begat, S. L., Podvin, P., and Lambare, G., 2003, Practical aspects and applications of 2D sterotomography: Geophysics, **68**, no. 3, 1008–1021.

Biondi, B., and Sava, P., 1999, Wave-equation migration velocity analysis: Soc. of Expl. Geophys., 69th Ann. Internat. Mtg, 1723–1726.

Biondi, B., Fomel, S., and Alkhalifah, T., 1997, "Focusing" eikonal equation and global tomography: SEP–**95**, 61–76.

Brown, M., 2002, Simultaneous estimation of two slopes from seismic data, applied to signal/noise separation: SEP–**112**, 181–194.

Clapp, R., and Biondi, B., 2000, Tau domain migration velocity analysis using angle CRP gathers and geologic constrains: Soc. of Expl. Geophys., 70th Ann. Internat. Mtg, 926–929.

Clapp, R. G., 2001, Geologically constrained migration velocity analysis: Ph.D. thesis, Stanford University.

Etgen, J., 1990, Residual prestack migration and interval velocity estimation: Ph.D. thesis, Stanford University.

Fomel, S., 2002, Applications of plane-wave destruction filters: Geophysics, **67**, no. 06, 1946–1960.

Lomask, J., and Guitton, A., 2004, Analytical flattening with adjustable regularization: SEP–**115**, 367–382.

Lomask, J., 2003, Flattening 3D seismic cubes without picking: Soc. of Expl. Geophys., 73rd Ann. Internat. Mtg., 1402–1405.

Symes, W. W., and Carazzone, J. J., 1991, Velocity inversion by differential semblance optimization: Geophysics, **56**, no. 05, 654–663.

Toldi, J. L., 1989, Velocity analysis without picking: Geophysics, **54**, no. 02, 191–199.